VIBRATION CALCULATION OF SPATIAL MULTIBODY SYSTEMS BASED ON CONSTRAINT-TOPOLOGY TRANSFORMATION

W. Jiang [*] **X. D. Chen** [**] **X. Luo** [***]

State Key Laboratory of Digital Manufacturing Equipment & Technology
Huazhong University of Science and Technology
Wuhan 430074, China

Y. T. Hu [****] **H. P. Hu** [***]

Department of Mechanics
Huazhong University of Science and Technology
Wuhan 430074, China

ABSTRACT

Many kinds of mechanical systems can be modeled as spatial rigid multibody systems (SR-MBS), which consist of a set of rigid bodies interconnected by joints, springs and dampers. Vibration calculation of SR-MBS is conventionally conducted by approximately linearizing the nonlinear equations of motion and constraint, which is very complicated and inconvenient for sensitivity analysis. A new algorithm based on constraint-topology transformation is presented to derive the oscillatory differential equations in three steps, that is, vibration equations for free SR-MBS are derived using Lagrangian method at first; then, an open-loop constraint matrix is derived to obtain the vibration equations for open-loop SR-MBS via quadric transformation; finally, a cut-joint constraint matrix is derived to obtain the vibration equations for closed-loop SR-MBS via quadric transformation. Through mentioned above, the vibration calculation can be significantly simplified and the sensitivity analysis can be conducted conveniently. The correctness of the proposed method has been verified by numerical experiments in comparison with the traditional approaches.

Keywords: Multibody system, Vibration calculation, Constraint-topology transformation.

1. INTRODUCTION

Many kinds of mechanical systems are often modeled as spatial rigid multibody systems (SR-MBS), such as robots, machine tools, automobiles and aircrafts. An SR-MBS typically consists of a set of rigid bodies interconnected by kinematic constraints and force elements in spatial configuration [1]. Each flexible body can be further modeled as a set of rigid bodies interconnected by kinematic constraints and force elements [2]. Dynamic modeling and vibration analysis based on multibody dynamics are essential to design, optimization and control of these systems [3,4]. Vibration calculation of SR-MBS are usually started by solving large-scale nonlinear equations of motion combined with constraint equations [5], and then linearization is carried out to obtain a set of linearized differential-algebraic equations (DAEs) or second-order ordinary differential equations (ODEs) [6-10]. This kind of method is necessary for solving the dynamics of nonlinear systems with large deformation.

However, there are two major disadvantages for vibration calculation of SR-MBS by using the conventional method. On the one hand, the computational efficiency is very low due to a large amount of efforts usually required for computation of trigonometric functions, derivation and linearization. Many approaches have been proposed to simplify the formulation, such as proper selection of reference frames [11], generalized coordinates [12-15], mechanics principles [16,17], and other methods [18,19]. On the other hand, despite sensitivity analysis of SR-MBS based on the conventional method is well documented [20-24], the formulation is quite complicated because the resulting equations are implicit functions of the design parameters.

Actually, what people concern, for many kinds of mechanical systems under working conditions, are eigenvalue problems and the relationship between the modal parameters and the design parameters. And the designer needs to know the results as quickly as possible so as to perform optimal design. From this point of view, fast algorithm for vibration calculation and sensitivity analysis with easiness of application is critical to the design of a complex mechanical system. A

[*] Postdoctoral Researcher [**] Professor, corresponding author [***] Associate Professor [****] Professor

DOI : 10.1017/jmech.2011.51
Copyright © 2011 The Society of Theoretical and Applied Mechanics, R.O.C.
https://doi.org/10.1017/jmech.2011.51 Published online by Cambridge University Press

novel formulation based on matrix transformation for open-loop rigid multibody systems has been proposed recently [25]. The algorithm has been further improved to directly generate the open-loop constraint matrix instead of matrix multiplication [26]. The computational efficiency has been significantly improved, and the resulting equations are explicit functions of the design parameters that can be easily applied for sensitivity analysis. Particularly, the proposed method can be used to directly obtain sensitivity of system matrices about design parameters which are required to perform mode shape sensitivity analysis [27,28].

Vibration calculation of general SR-MBS containing closed-loop constraints is investigated in this article. Vibration displacements of bodies are selected as generalized coordinates. The translational and rotational displacements are integrated in spatial notation. Linear transformation of vibration displacements between different points on the same rigid body is derived. Absolute joint displacement is introduced to give mathematical definition for ideal joint in a new form. Constraint equations written in this way can be solved easily via the proposed linear transformation. A new formulation based on constraint-topology transformation is proposed to generate oscillatory differential equations for a general SR-MBS, by matrix generation and quadric transformation in three steps:

1. Linearized ODEs in terms of absolute displacements are firstly derived by using Lagrangian method for free SR-MBS without considering any constraint.
2. An open-loop constraint matrix $\boldsymbol{B}'$ is derived to formulate linearized ODEs via quadric transformation $\boldsymbol{E}' = \boldsymbol{B}'^{T}\boldsymbol{E}\boldsymbol{B}'(\boldsymbol{E} = \boldsymbol{M}, \boldsymbol{K}, \boldsymbol{C})$ for open-loop SR-MBS, which is obtained from closed-loop SR-MBS by using cut-joint method.
3. A constraint matrix $\boldsymbol{B}''$ corresponding to all cut-joints is finally derived to formulate a minimal set of ODEs via quadric transformation $\boldsymbol{E}'' = \boldsymbol{B}''^{T}\boldsymbol{E}'\boldsymbol{B}''(\boldsymbol{E} = \boldsymbol{M}, \boldsymbol{K}, \boldsymbol{C})$ for closed-loop SR-MBS.

Complicated solving for constraints and linearization are unnecessary for the proposed method, therefore the procedure of vibration calculation can be greatly simplified. In addition, since the resulting equations are explicit functions of the design parameters, the suggested method is particularly suitable for sensitivity analysis and optimization for large-scale SR-MBS, which is very difficult to be achieved by using conventional approaches.

A T-shape cantilever beam and a Stewart isolation platform, which represent tree and closed-loop SR-MBS, are taken as case studies to verify the proposed method. Comparisons with traditional approaches show that the results of vibration calculation by using the proposed method are accurate.

2. DESCRIPTION OF SR-MBS

As shown in Fig. 1, considering an SR-MBS which consists of n rigid bodies and the ground B_0, each two

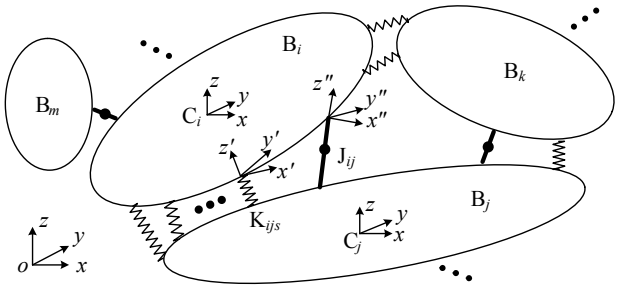


Fig. 1. Elements and reference frames in SR-MBS

bodies are probably interconnected by at most one joint and/or arbitrary number of spatial spring-dampers. A spatial spring-damper means an integration of three spring-dampers and three torsional spring-dampers. Each joint contains at least one and at most six holonomic constraints. B_i denotes the i^{th} rigid body, and J_{ij} is the joint between B_i and B_j, where $i, j = 1, 2, \cdots, n$ and $i \neq j$. s_{ij} denotes the total number of spring-dampers between B_i and B_i, among which K_{ijs} is the s^{th} one, where $s = 0, 1, 2, \cdots, s_{ij}$. $s_{ij} = 0$ means there is no spring-damper between B_i and B_j.

Four kinds of reference frames are used in the formulation. The global reference frame, namely the inertial frame, *i.e.*, o - xyz, is fixed on the ground. The body reference frame, *e.g.*, c_i - xyz for B_i, is fixed in the space with its origin coinciding with the center of mass (CM) of the body. For simplicity without loss of generality, all body reference frames are set to be parallel to o - xyz in this paper. The spring reference frame, *e.g.*, u_{ijs} - $x'y'z'$ for K_{ijs}, is located at one of the spring acting points. The joint reference frame, *e.g.*, v_{ij} - $x''y''z''$ for J_{ij}, is located at one of the joint acting points.

The mass matrix of body B_i with respect to c_i - xyz is given by

$$\boldsymbol{M}_i = diag(m_i \boldsymbol{I} \quad \boldsymbol{J}_i)$$

where m_i is the mass of B_i, $\boldsymbol{J}_i$ is the inertia tensor of B_i with respect to c_i - xyz, and $\boldsymbol{I}$ is a 3×3 identity matrix.

The mass matrix of the free SR-MBS can be organized as

$$\boldsymbol{M} = \mathrm{diag}(\boldsymbol{M}_1 \quad \boldsymbol{M}_2 \quad \cdots \quad \boldsymbol{M}_n) \tag{1}$$

The translation of CM of B_i is specified via vector $r_i = [x_i\ y_i\ z_i]^{\mathrm{T}}$. The rotation of B_i is specified via Bryan angles $\theta_i = [\alpha_i\ \beta_i\ \gamma_i]^{\mathrm{T}}$. The absolute angular velocities can be expressed as [3]

$$\boldsymbol{\omega}_i = \begin{bmatrix} \omega_{ix} \\ \omega_{iy} \\ \omega_{iz} \end{bmatrix} = \begin{bmatrix} C_{\beta i}\, C_{\gamma i} & S_{\gamma i} & 0 \\ -C_{\beta i}\, S_{\gamma i} & C_{\gamma i} & 0 \\ S_{\beta i} & 0 & 1 \end{bmatrix} \begin{bmatrix} \dot{\alpha}_i \\ \dot{\beta}_i \\ \dot{\gamma}_i \end{bmatrix} \tag{2}$$

where $S_\mu = \sin\mu$, $C_\mu = \cos\mu (\mu = \alpha_i, \beta_i, \gamma_i)$.

Due to small angular displacements of bodies, *i.e.*, α_i, β_i, $\gamma_i \approx 0$, the absolute angular velocities and displacements can be linearized as [3]

$$\boldsymbol{\omega}_i \approx [\dot{\alpha}_i \quad \dot{\beta}_i \quad \dot{\gamma}_i]^{\mathrm{T}} = \dot{\boldsymbol{\theta}}_i \tag{3}$$

https://doi.org/10.1017/jmech.2011.51 Published online by Cambridge University Press

$$\Theta = \int \boldsymbol{\omega}_i \, \mathrm{d}t \approx \int \dot{\boldsymbol{\theta}}_i \, \mathrm{d}t = \boldsymbol{\theta}_i \tag{4}$$

The spatial displacements of B_i can be unified as

$$\boldsymbol{q}_i = [\boldsymbol{r}_i^T \quad \boldsymbol{\theta}_i^T]^T = [x_i \quad y_i \quad z_i \quad \alpha_i \quad \beta_i \quad \gamma_i]^T \tag{5}$$

The displacements and velocities for free SR-MBS can be organized as $\boldsymbol{q} = [\boldsymbol{q}_1^T \quad \boldsymbol{q}_2^T \quad \cdots \quad \boldsymbol{q}_n^T]^T$ and $\dot{\boldsymbol{q}} = [\dot{\boldsymbol{q}}_1^T \quad \dot{\boldsymbol{q}}_2^T \quad \cdots \quad \dot{\boldsymbol{q}}_n^T]^T$.

The stiffness and damping coefficients of K_{ijs} are defined in spring reference frame u_{ijs} - $x'y'z'$ as

$$\boldsymbol{K}_{ijs}^u = \mathrm{diag}\,(k_x \quad k_y \quad k_z \quad k_\alpha \quad k_\beta \quad k_\gamma)$$

$$\boldsymbol{C}_{ijs}^u = \mathrm{diag}\,(c_x \quad c_y \quad c_z \quad c_\alpha \quad c_\beta \quad c_\gamma)$$

P_{ijs} and P_{jis} are the acting points of K_{ijs} on B_i and B_j. $\bar{\boldsymbol{r}}_{ijs} = [\bar{x}_{ijs} \quad \bar{y}_{ijs} \quad \bar{z}_{ijs}]^T$ denotes the original position of P_{ijs} relative to c_i - xyz. $\bar{\boldsymbol{r}}_{jis} = [\bar{x}_{jis} \quad \bar{y}_{jis} \quad \bar{z}_{jis}]^T$ denotes the original position of P_{jis} relative to c_j - xyz. $\bar{\boldsymbol{\theta}}_{ijs} = [\bar{\alpha}_{ijs} \quad \bar{\beta}_{ijs} \quad \bar{\gamma}_{ijs}]^T$ denotes the original orientation of K_{ijs} relative to c_i - xyz.

Most of the joints that used for practical applications can be modeled in terms of the so-called lower pairs, including revolute, prismatic, cylindrical, universal, spherical, and planar joints. Each joint reduces corresponding number of degrees of freedom (DOFs) of the distal body [6,29] between two connected bodies. Assume there is an ideal joint J_{ij} between body B_i and B_j. The acting points of J_i on B_i and B_j are marked as Q_{ij} and Q_{ji}, respectively. $\bar{\boldsymbol{r}}_{ijq} = [\bar{x}_{ijq} \quad \bar{y}_{ijq} \quad \bar{z}_{ijq}]^T$ denotes the original position of Q_{ij} relative to c_i - xyz. $\bar{\boldsymbol{r}}_{jiq} = [\bar{x}_{jiq} \quad \bar{y}_{jiq} \quad \bar{z}_{jiq}]^T$ denotes the original position of Q_{ji} relative to c_j - xyz. $\bar{\boldsymbol{\theta}}_{ij} = [\bar{\alpha}_{ij} \quad \bar{\beta}_{ij} \quad \bar{\gamma}_{ij}]^T$ denotes the original orientation of J_{ij} relative to c_i - xyz. $\boldsymbol{q}_{ij}^v$ and $\boldsymbol{q}_{ji}^v$ are absolute joint displacements of Q_{ij} and Q_{ji} with respect to v_{ij} - $x''y''z''$. A 6×6 diagonal matrix $\boldsymbol{H}$ is introduced for each kind of joint to formulate the constraint equations in terms of absolute joint displacements. For example, the constraint equations for joint J_{ij} can be written as

$$\boldsymbol{H}_{ij} \, \boldsymbol{q}_{ij}^v = \boldsymbol{H}_{ij} \, \boldsymbol{q}_{ji}^v$$

The meaning of matrix $\boldsymbol{H}$ can be explained as follows: The value of each diagonal element in $\boldsymbol{H}$ is either one or zero, representing whether the DOF along the corresponding axis is constrained or not. In order to reduce the number of constraint equations, another matrix $\boldsymbol{D}$ is introduced for each kind of joint to extract the independent variables, *e.g.*, for joint J_{ij} it turns to be $\boldsymbol{q}_j' = \boldsymbol{D}_{ij} \, \boldsymbol{q}_{qji}^v$. Matrix $\boldsymbol{D}$ is obtained from matrix $\boldsymbol{I} - \boldsymbol{H}$ by removing those rows whose elements are all zero. Matrices for some common joints are shown in Table 1.

Transmission mechanisms are another kind of constraints widely used in mechanical systems, such as gear pair, rackandpinion, worm gear pair, screw pair, *etc*. They are usually related to a pair of joints, therefore the constraint equations can be written in terms of absolute joint displacements. Suppose there is a transmission mechanism T_{kr} between body B_k and B_r, T_{kr} is related to joint J_{jk} and J_{mr}. The joint acting point of J_{jk} on B_k is marked as Q_{jk}, and that of J_{mr} on B_r is marked as Q_{mr}. The constraint equations for T_{kr} can be expressed as

$$\boldsymbol{G}_k \, \boldsymbol{q}_{jk}^v + \boldsymbol{G}_r \, \boldsymbol{q}_{mr}^v = \boldsymbol{0} \tag{6}$$

where $\boldsymbol{q}_{jk}^v$ is the absolute joint displacement of Q_{jk} with respect to v_{jk} - $x''y''z''$, and $\boldsymbol{q}_{mr}^v$ is that of Q_{mr} with respect to v_{mr} - $x''y''z''$. Matrices $\boldsymbol{G}_k$ and $\boldsymbol{G}_r$ are used to extract variables relative to transmission mechanism. Matrices for some common transmission mechanisms are shown in Table 2, in which i is the transmission ratio.

Table 1 Mathematical definition of some common joints

Joint type	Free axes	Matrix $\boldsymbol{H}$	Matrix $\boldsymbol{D}$
Fixed	none	$\boldsymbol{I}_6$	null matrix
revolute	γ	diag (1 1 1 1 1 0)	[0 0 0 0 0 1]
prismatic	Z	diag (1 1 0 1 1 1)	[0 0 1 0 0 0]
cylindrical	Z, γ	diag (1 1 0 1 1 0)	$\begin{bmatrix} 0&0&1&0&0&0 \\ 0&0&0&0&0&1 \end{bmatrix}$
universal	α, β	diag (1 1 1 0 0 1)	$\begin{bmatrix} 0&0&0&1&0&0 \\ 0&0&0&0&1&0 \end{bmatrix}$
spherical	α, β, γ	diag (1 1 1 0 0 0)	$\begin{bmatrix} 0&0&0&1&0&0 \\ 0&0&0&0&1&0 \\ 0&0&0&0&0&1 \end{bmatrix}$
planar	x, y, γ	diag (0 0 1 1 1 0)	$\begin{bmatrix} 1&0&0&0&0&0 \\ 0&1&0&0&0&0 \\ 0&0&0&0&0&1 \end{bmatrix}$
…	…	…	…

3. LINEAR TRANSFORMATION OF VIBRATION DISPLACEMENTS

Transformation of displacements of two points on a same rigid body is fundamental to the dynamics of an SR-MBS. The transformation can be divided into two steps. Firstly, the displacements of spring acting point are formulated by using the displacements of CM on the same body, with respect to the same reference frame. And then the resulting displacements are transformed from body reference frame to spring reference frame. A linear transformation is proposed for vibration displacements based on homogeneous transformation.

Assume that there are two reference frames, c - xyz and u - $x'y'z'$. The direction cosine matrix from c - xyz to u - $x'y'z'$ is determined by $\theta = [\alpha \ \beta \ \gamma]^T$ as follows

https://doi.org/10.1017/jmech.2011.51 Published online by Cambridge University Press

Table 2 Mathematical definition of some transmission mechanisms

Transmission	Constraint equation	Matrix $\boldsymbol{G}_1$	Matrix $\boldsymbol{G}_2$
Gear pair	$\hat{\gamma}_1 + i\,\hat{\gamma}_2 = 0$	[0 0 0 0 0 1]	[0 0 0 0 0 i]
Worm gear pair	$\hat{\gamma}_1 + i\,\hat{\gamma}_2 = 0$	[0 0 0 0 0 1]	[0 0 0 0 0 i]
Rackand-pinion	$\hat{\gamma}_1 + i\,\hat{z}_2 = 0$	[0 0 0 0 0 1]	[0 0 I 0 0 0]
Screw pair	$\hat{\gamma}_1 + i\,\hat{z}_1 - i\,\hat{z}_2 = 0$	[0 0 i 0 0 1]	[0 0 $-i$ 0 0 0]
…	…	…	…

$$\boldsymbol{A}^{cu} = \begin{bmatrix} \mathrm{C}_\beta \mathrm{C}_\gamma & \mathrm{C}_\alpha \mathrm{S}_\gamma + \mathrm{S}_\alpha \mathrm{S}_\beta \mathrm{C}_\gamma & \mathrm{S}_\alpha \mathrm{S}_\gamma - \mathrm{C}_\alpha \mathrm{S}_\beta \mathrm{C}_\gamma \\ -\mathrm{C}_\beta \mathrm{S}_\gamma & \mathrm{C}_\alpha \mathrm{C}_\gamma - \mathrm{S}_\alpha \mathrm{S}_\beta \mathrm{S}_\gamma & \mathrm{S}_\alpha \mathrm{C}_\gamma + \mathrm{C}_\alpha \mathrm{S}_\beta \mathrm{S}_\gamma \\ \mathrm{S}_\beta & -\mathrm{S}_\alpha \mathrm{C}_\beta & \mathrm{C}_\alpha \mathrm{C}_\beta \end{bmatrix} \quad (7)$$

where $S_\mu = \sin\mu$, $C_\mu = \cos\mu(\mu = \alpha, \beta, \gamma)$.

The translational and rotational displacements can be integrated as spatial vector and the transformation between different reference frames can be expressed as

$$\boldsymbol{q}_C^u = \begin{bmatrix} \boldsymbol{r}_C^u \\ \boldsymbol{\theta}_C^u \end{bmatrix} = \begin{bmatrix} \boldsymbol{A}^{cu} & \boldsymbol{0} \\ \boldsymbol{0} & \boldsymbol{A}^{cu} \end{bmatrix} \begin{bmatrix} \boldsymbol{r}_C^c \\ \boldsymbol{\theta}_C^c \end{bmatrix} = \boldsymbol{R}^{cu} \boldsymbol{q}_C^c \quad (8)$$

Suppose C and P are two different points on a same rigid body. As shown in Fig. 2, $\overline{\boldsymbol{r}}_{CP} = [\overline{x}_{CP} \;\; \overline{y}_{CP} \;\; \overline{z}_{CP}]^T$ denotes the position of P relative to C. $\boldsymbol{q}_C = [\boldsymbol{r}_C^T \;\; \boldsymbol{\theta}_C^T]^T$ denotes the vector of displacements of point C. Notice that point mentioned in this paper is actually mark that has angular displacements. The translational displacements of point P can be expressed as

$$\begin{aligned} \boldsymbol{r}_P &= \overline{\boldsymbol{r}}_{OP'} - \overline{\boldsymbol{r}}_{OP} \\ &= \overline{\boldsymbol{r}}_{OC} + \boldsymbol{r}_C + \overline{\boldsymbol{r}}_{C'P'} - (\overline{\boldsymbol{r}}_{OC} + \overline{\boldsymbol{r}}_{CP}) \\ &= \boldsymbol{r}_C + A^{-1}\,\overline{\boldsymbol{r}}_{CP} - \overline{\boldsymbol{r}}_{CP} \\ &= \boldsymbol{r}_C + (A^T - I)\,\overline{\boldsymbol{r}}_{CP} \end{aligned} \quad (9)$$

The rotational displacements of different points on a same rigid body are equal to each other, *i.e.*, $\boldsymbol{\theta}_P = \boldsymbol{\theta}_C$. It means that the translational and rotational displacements of point P can be integrated as

$$\boldsymbol{q}_P = \begin{bmatrix} \boldsymbol{r}_P \\ \boldsymbol{\theta}_P \end{bmatrix} = \begin{bmatrix} \boldsymbol{r}_C + (\boldsymbol{A}^T - \boldsymbol{I})\,\overline{\boldsymbol{r}}_{CP} \\ \boldsymbol{\theta}_C \end{bmatrix} \quad (10)$$

Due to small angular displacements for vibration analysis, *i.e.*, $\alpha, \beta, \gamma \approx 0$, the direction cosine matrix in Eq. (7) can be linearized as [3,13,26]

$$\boldsymbol{A} \approx \begin{bmatrix} 1 & \gamma & -\beta \\ -\gamma & 1 & \alpha \\ \beta & -\alpha & 1 \end{bmatrix} \quad (11)$$

Substitute Eq. (11) into Eq. (9), it yields

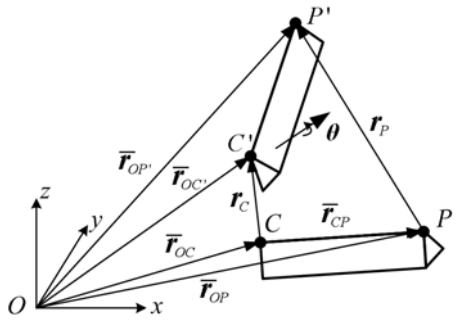


Fig. 2 Finite displacements of two points on a same rigid body

$$\begin{aligned} (\boldsymbol{A}^T - \boldsymbol{I})\,\overline{\boldsymbol{r}}_{CP} &\approx \begin{bmatrix} 0 & -\gamma & \beta \\ \gamma & 0 & -\alpha \\ -\beta & \alpha & 0 \end{bmatrix} \begin{bmatrix} \overline{x}_{CP} \\ \overline{y}_{CP} \\ \overline{z}_{CP} \end{bmatrix} \\ &= \begin{bmatrix} 0 & -\overline{z}_{CP} & \overline{y}_{CP} \\ \overline{z}_{CP} & 0 & -\overline{x}_{CP} \\ -\overline{y}_{CP} & \overline{x}_{CP} & 0 \end{bmatrix} \begin{bmatrix} \alpha \\ \beta \\ \gamma \end{bmatrix} \\ &= \mathbf{U}_{CP}\,\boldsymbol{\theta}_C \end{aligned} \quad (12)$$

Therefore Eq. (10) can be linearized to formulate the relationship between fine displacements of two points on a same rigid body as follows

$$\boldsymbol{q}_P \approx \begin{bmatrix} \boldsymbol{I} & \boldsymbol{U}_{CP} \\ \boldsymbol{0} & \boldsymbol{I} \end{bmatrix} \boldsymbol{q}_C = \boldsymbol{T}_{CP}\,\boldsymbol{q}_C \quad (13)$$

According to description in Section 2, the displacements of spring acting point P_{ijs} in u_{ijs} - $x'y'z'$ can be figured out using fine displacements of CM on the same body in c - xyz as follows

$$\boldsymbol{q}_{ijs}^u = \boldsymbol{R}_{ijs}^{cu}\,\boldsymbol{T}_{ijs}\,\boldsymbol{q}_i \quad (14)$$

where $\boldsymbol{R}_{ijs}^{cu}$ can be formulated using $\overline{\boldsymbol{\theta}}_{ijs}$ according to Eqs. (7) and (8), and $\boldsymbol{T}_{ijs}$ can be formulated using $\overline{\boldsymbol{r}}_{ijs}$ according to Eqs. (12) and (13).

Similarly, displacements of joint acting point Q_{ij} in v_{ij} - $x''y''z''$ can be expressed as

$$\boldsymbol{q}_{ij}^v = \boldsymbol{R}_{ij}^{cv}\,\boldsymbol{T}_{ij}\,\boldsymbol{q}_i \quad (15)$$

where $\boldsymbol{R}_{ij}^{cv}$ can be formulated using $\overline{\boldsymbol{\theta}}_{ij}$ according to Eqs. (7) and (8), and $\boldsymbol{T}_{ij}$ can be formulated using $\overline{\boldsymbol{r}}_{ij}$ according to Eqs. (12) and (13).

4. VIBRATION FORMULATION OF SR-MBS

Generally, there might be none or more then one joint in a SR-MBS. As shown in Fig. 3, the topologies of constraints in multibody systems can be classified into five groups: (a) free, (b) scattered, (c) chain, (d) tree, and (e) closed-loop. Free SR-MBS means that there is no constraint in the system. Groups (b), (c) and (d) can all be regarded as general open-loop SR-

https://doi.org/10.1017/jmech.2011.51 Published online by Cambridge University Press

MBS. Since the spring-dampers do not change the topology of constraints in an SR-MBS, spring-dampers between two nonadjacent bodies are not displayed in the figure.

Considering a general closed-loop SR-MBS as shown in Fig. 3(e), body B_i, B_j, B_k and are B_r are connected with joints J_{ij}, J_{jk} and J_{rk}, whereas B_j, B_m and B_r are connected with joints J_{jm} and J_{mr}. Without loss of generality, assume that $1 \le i < j < k < m < r \le n$. Firstly, linearized ODEs in terms of absolute displacements are derived by using Lagrangian method for free SR-MBS without considering any constraint, as shown in Fig. 3(a). Secondly, an open-loop constraint matrix is derived to formulate linearized ODEs via quadric transformation for open-loop SR-MBS, which is obtained by ignoring all cut-joints [6,29], *e.g.*, if J_{kr} is chosen as cut-joint and one can obtain open-loop SR-MBS as shown in Fig. 3(d). Finally, a cut-joint constraint matrix corresponding to all cut-joints is solved to formulate a minimal set of ODEs via quadric transformation for closed-loop SR-MBS.

4.1 Vibration Formulation of Free SR-MBS

The total kinetic energy of the system as shown in Fig. 3(a) is the summation of translational energy and rotational energy of all bodies, *i.e.*,

$$T = \sum_{i=1}^{n}\left(\frac{1}{2}\dot{\boldsymbol{r}}_i^T m_i \dot{\boldsymbol{r}}_i + \frac{1}{2}\boldsymbol{\omega}_i^T \boldsymbol{J}_i \boldsymbol{\omega}_i\right) \approx \sum_{i=1}^{n}\frac{1}{2}\dot{\boldsymbol{q}}_i^T \boldsymbol{M}_i \dot{\boldsymbol{q}}_i \tag{16}$$

The fine deformation of spring K_{ijs} can be formulated as difference of displacements between P_{ijs} and P_{jis} in u_{ijs} - $x'y'z'$

$$\Delta\boldsymbol{q}_{ijs}^u = \boldsymbol{q}_{jis}^u - \boldsymbol{q}_{ijs}^u = \boldsymbol{R}_{ijs}^{cu}\boldsymbol{T}_{jis}\boldsymbol{q}_j - \boldsymbol{R}_{ijs}^{cu}\boldsymbol{T}_{ijs}\boldsymbol{q}_i \tag{17}$$

Set the potential energy of the system at equilibrium positions to be zero. Then the potential energy of spring K_{ijs} can be formulated as

$$V_{ijs} = \frac{1}{2}(\Delta\boldsymbol{q}_{ijs}^u)^{\mathrm{T}}\boldsymbol{K}_{ijs}^u\Delta\boldsymbol{q}_{ijs}^u \tag{18}$$

The potential energy of the entire system is the sum of gravitational potential V_g and elastic potential V_k, *i.e.*,

$$V = V_g + V_k = \sum_{i=0}^{n}\boldsymbol{q}_i^T\boldsymbol{M}_i\boldsymbol{g} + \sum_{i=0}^{n-1}\sum_{j=i+1}^{n}\sum_{s=0}^{s_{ij}}V_{ijs} \tag{19}$$

where $\boldsymbol{g} = [0\ 0\ g\ 0\ 0\ 0]^T$ is the vector of gravitational acceleration. Since there might be no spring-damper between two bodies, a "virtual spring-damper" which has no effect on the system is introduced between each two bodies for consistency in formula. For example, K_{ij0} is the "virtual spring-damper" between body B_i and B_j, and $\boldsymbol{K}_{ij0}^u = \boldsymbol{0}$, $\boldsymbol{C}_{ij0}^u = \boldsymbol{0}$.

The Lagrangian equations of the system take the form

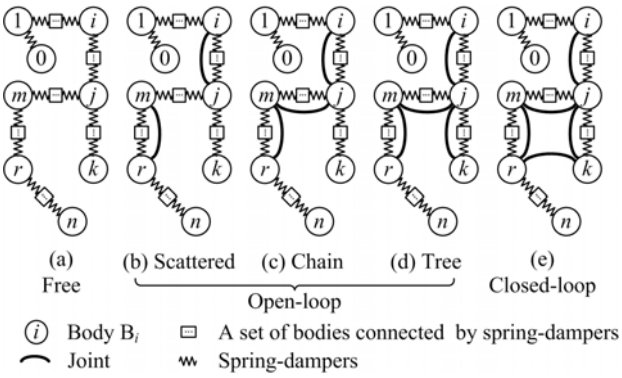


Fig. 3 Topologies of constraints in SR-MBS

$$\frac{d}{dt}\left(\frac{\partial T}{\partial\dot{\boldsymbol{q}}_i^T}\right) - \frac{\partial V}{\partial\boldsymbol{q}_i^T} = \boldsymbol{f}_{di} + \boldsymbol{f}_{ei} \tag{20}$$

where $i = 1, 2, \cdots, n$, $\boldsymbol{f}_{di}$ and $\boldsymbol{f}_{ei}$ denote the damping forces and other non-potential forces acting on body B_i.

Due to property $\boldsymbol{M}_i^T = \boldsymbol{M}_i$, it yields

$$\frac{d}{dt}\left(\frac{\partial T}{\partial\dot{\boldsymbol{q}}_i^T}\right) = \frac{1}{2}(\boldsymbol{M}_i + \boldsymbol{M}_i^T)\ddot{\boldsymbol{q}}_i = \boldsymbol{M}_i\ddot{\boldsymbol{q}}_i \tag{21}$$

Substitute Eqs. (17) and (18) into Eq. (19), and partially derivate V with respect to $\boldsymbol{q}_i^T$, it yields

$$\begin{aligned}
\frac{\partial V}{\partial\boldsymbol{q}_i^T} &= \sum_{k=0,k\neq i}^{n}\frac{\partial\boldsymbol{q}_k^T}{\partial\boldsymbol{q}_i^T}\boldsymbol{M}_k\boldsymbol{g} + \frac{\partial\boldsymbol{q}_i^T}{\partial\boldsymbol{q}_i^T}\boldsymbol{M}_i\boldsymbol{g} \\
&\quad + \sum_{k=0}^{i-1}\sum_{s=0}^{s_{ki}}\frac{\partial V_{kis}}{\partial\boldsymbol{q}_i^T} + \sum_{j=i+1}^{n}\sum_{s=0}^{s_{ij}}\frac{\partial V_{ijs}}{\partial\boldsymbol{q}_i^T} + \sum_{k=i+1}^{n-1}\sum_{j=k+1}^{n}\sum_{s=0}^{s_{kj}}\frac{\partial V_{kjs}}{\partial\boldsymbol{q}_i^T} \\
&= \boldsymbol{0} + \boldsymbol{M}_i\boldsymbol{g} + \sum_{j=0}^{i-1}\sum_{s=0}^{s_{ij}}\frac{\partial V_{ijs}}{\partial\boldsymbol{q}_i^T} + \sum_{j=i+1}^{n}\sum_{s=0}^{s_{ij}}\frac{\partial V_{ijs}}{\partial\boldsymbol{q}_i^T} + \boldsymbol{0} \\
&= \boldsymbol{M}_i\boldsymbol{g} + \sum_{j=0,j\neq i}^{n}\sum_{s=0}^{s_{ij}}\frac{\partial V_{ijs}}{\partial\boldsymbol{q}_i^T} \\
&= \boldsymbol{M}_i\boldsymbol{g} + \sum_{j=0,j\neq i}^{n}\sum_{s=}^{s_{ij}}\left\{(\boldsymbol{T}_{ijs})^T(\boldsymbol{R}_{ijs}^{cu})^T\boldsymbol{K}_{ijs}^u\boldsymbol{R}_{ijs}^{cu}(\boldsymbol{T}_{ijs}\boldsymbol{q}_i - \boldsymbol{T}_{jis}\boldsymbol{q}_j)\right\} \\
&= \boldsymbol{M}_i\boldsymbol{g} + \left[\sum_{j=0,j\neq i}^{n}\sum_{s=}^{s_{ij}}(\boldsymbol{T}_{ijs})^T(\boldsymbol{R}_{ijs}^{cu})^T\boldsymbol{K}_{ijs}^u\boldsymbol{R}_{ijs}^{cu}\boldsymbol{T}_{ijs}\right]\boldsymbol{q}_i \\
&\quad - \sum_{j=0,j\neq i}^{n}\left[\sum_{s=}^{s_{ij}}(\boldsymbol{T}_{ijs})^T(\boldsymbol{R}_{ijs}^{cu})^T\boldsymbol{K}_{ijs}^u\boldsymbol{R}_{ijs}^{cu}\boldsymbol{T}_{jis}\boldsymbol{q}_j\right]
\end{aligned} \tag{22}$$

Denote

$$\boldsymbol{E}_{ii} = \sum_{j=0,j\neq i}^{n}\sum_{s=0}^{s_{ij}}(\boldsymbol{T}_{ijs})^{\mathrm{T}}(\boldsymbol{R}_{ijs}^{cu})^{\mathrm{T}}\boldsymbol{E}_{ijs}^u\boldsymbol{R}_{ijs}^{cu}\boldsymbol{T}_{ijs} \tag{23}$$

$$\boldsymbol{E}_{ij} = \sum_{s=0}^{s_{ij}}(\boldsymbol{T}_{ijs})^{\mathrm{T}}(\boldsymbol{R}_{ijs}^{cu})^{\mathrm{T}}\boldsymbol{E}_{ijs}^u\boldsymbol{R}_{ijs}^{cu}\boldsymbol{T}_{jis} \tag{24}$$

Let $\boldsymbol{E} = \boldsymbol{K}$, then Eq. (22) can be rewritten as

$$\frac{\partial V}{\partial\boldsymbol{q}_i^{\mathrm{T}}} = \boldsymbol{K}_{ii}\boldsymbol{q}_i - \sum_{j=0,j\neq i}^{n}\boldsymbol{K}_{ij}\boldsymbol{q}_j + \boldsymbol{M}_i\boldsymbol{g} \tag{25}$$

https://doi.org/10.1017/jmech.2011.51 Published online by Cambridge University Press

The dissipation power due to damping forces can be formulated as [2]

$$P=-\sum_{i=0}^{n-1}\sum_{j=i+1}^{n}\sum_{s=0}^{s_{ij}}\frac{1}{2}(\Delta\dot{\boldsymbol{q}}_{ijs}^{u})^{\mathrm{T}}\boldsymbol{C}_{ijs}^{u}\Delta\dot{\boldsymbol{q}}_{ijs}^{u} \tag{26}$$

Similarly, the damping forces acting on B_i with respect to c_i - xyz can be evaluated as

$$\boldsymbol{f}_{di}=\frac{\partial P}{\partial\dot{\boldsymbol{q}}_i^{\mathrm{T}}}=-\boldsymbol{C}_{ii}\dot{\boldsymbol{q}}_i+\sum_{j=0,j\neq i}^{n}\mathbf{C}_{ij}\dot{\boldsymbol{q}}_j \tag{27}$$

It can be proved that $\boldsymbol{C}_{ii}$ and $\boldsymbol{C}_{ij}$ are also determined by Eqs. (23) and (24) for $\boldsymbol{E}=\boldsymbol{C}$.

The linearized ODEs for a free SR-MBS turn to be

$$\boldsymbol{M}\ddot{\boldsymbol{q}}+\boldsymbol{C}\dot{\boldsymbol{q}}+\boldsymbol{K}\boldsymbol{q}=\boldsymbol{f}_e-\boldsymbol{f}_g \tag{28}$$

where quantities $\boldsymbol{f}_g=[(\boldsymbol{M}_1\boldsymbol{g})^T\ (\boldsymbol{M}_2\boldsymbol{g})^T\cdots(\boldsymbol{M}_n\boldsymbol{g})^T]^T$ and $\boldsymbol{f}_e=[\boldsymbol{f}_{e1}^T\ \ \boldsymbol{f}_{e2}^T\ \cdots\ \boldsymbol{f}_{en}^T]^T$ denote gravity forces and other non-potential forces. The damping matrix $\boldsymbol{C}$ and stiffness matrix $\boldsymbol{K}$ in Eq. (28) take the same form

$$\boldsymbol{E}=\begin{bmatrix}\boldsymbol{E}_{11} & -\boldsymbol{E}_{12} & \cdots & -\boldsymbol{E}_{1n}\\ -\boldsymbol{E}_{21} & \boldsymbol{E}_{22} & \cdots & \vdots\\ \vdots & \vdots & \ddots & -\boldsymbol{E}_{n-1,n}\\ -\boldsymbol{E}_{n1} & \cdots & -\boldsymbol{E}_{n,n-1} & \boldsymbol{E}_{nn}\end{bmatrix}\ (\boldsymbol{E}=\boldsymbol{C},\boldsymbol{K}) \tag{29}$$

$\boldsymbol{K}_{ii}$ and $\boldsymbol{C}_{ii}$ contain parameters of all springs and dampers that connected with B_i. $\boldsymbol{K}_{ij}$ and $\boldsymbol{C}_{ij}$ contain parameters of all springs and dampers that connected between B_i and B_j. Matrices $\boldsymbol{C}$ and $\boldsymbol{K}$ contain explicitly damping coefficients and stiffness coefficients, and reveal clearly the topology of spring-dampers.

Equations (16), (19) and (26) can be reformed as

$$T=\frac{1}{2}\dot{\boldsymbol{q}}^T\boldsymbol{M}\dot{\boldsymbol{q}} \tag{30}$$

$$V=\frac{1}{2}\boldsymbol{q}^T\boldsymbol{K}\boldsymbol{q}+\boldsymbol{q}^T\boldsymbol{f}_g \tag{31}$$

$$P=\frac{1}{2}\dot{\boldsymbol{q}}^T\boldsymbol{C}\dot{\boldsymbol{q}} \tag{32}$$

4.2 Vibration Formulation of Open-Loop SR-MBS

Select J_{rk} in Fig. 3(e) as cut-joint and one can obtain open-loop SR-MBS as shown in Fig. 3(d). The constraint equations for joint J_{ij} can be written as

$$\boldsymbol{H}_{ij}\boldsymbol{q}_{ij}^{v}=\boldsymbol{H}_{ij}\boldsymbol{R}_{ij}^{cv}\boldsymbol{T}_{ij}\boldsymbol{q}_i=\boldsymbol{H}_{ij}\boldsymbol{q}_{ji}^{v} \tag{33}$$

where $\boldsymbol{q}_{ij}^{v}$ and $\boldsymbol{q}_{ji}^{v}$ denote the displacements of joint acting points Q_{ij} and Q_{ji} with respect to v_{ij} - $x''y''z''$, respectively. $\boldsymbol{R}_{ij}^{cv}$ is determined by $\overline{\boldsymbol{\theta}}_{ij}$ according to Eqs. (7) and (8). $\boldsymbol{T}_{ij}$ is determined by $\overline{\boldsymbol{r}}_{ij}$ according to Eqs. (12) and (13). Due to properties $(\boldsymbol{I}-\boldsymbol{H}_{ij})\boldsymbol{D}_{ij}^{\mathrm{T}}\boldsymbol{D}_{ij}=\boldsymbol{I}-\boldsymbol{H}_{ij}$ and $(\boldsymbol{R}^{cv})^{-1}=\boldsymbol{R}^{vc}$, Eq. (33) can be reformed as

$$\begin{aligned}\boldsymbol{q}_j&=(\boldsymbol{T}_{ji})^{-1}\boldsymbol{R}_{ij}^{vc}\boldsymbol{H}_{ij}\boldsymbol{R}_{ij}^{cv}\boldsymbol{T}_{ij}\boldsymbol{q}_i+(\boldsymbol{T}_{ji})^{-1}\boldsymbol{R}_{ij}^{vc}(\boldsymbol{I}-\boldsymbol{H}_{ij})\boldsymbol{q}_{ji}^{v}\\&=(\boldsymbol{T}_{ji})^{-1}\boldsymbol{R}_{ij}^{vc}\boldsymbol{H}_{ij}\boldsymbol{R}_{ij}^{cv}\boldsymbol{T}_{ij}\boldsymbol{q}_i+(\boldsymbol{T}_{ji})^{-1}\boldsymbol{R}_{ij}^{vc}(\boldsymbol{I}-\boldsymbol{H}_{ij})\boldsymbol{D}_{ij}^{\mathrm{T}}\boldsymbol{D}_{ij}\boldsymbol{q}_{ji}^{v}\end{aligned} \tag{34}$$

Define

$$\boldsymbol{P}_{ij}=(\boldsymbol{T}_{ji})^{-1}\boldsymbol{R}_{ij}^{vc}\boldsymbol{H}_{ij}\boldsymbol{R}_{ij}^{cv}\boldsymbol{T}_{ij}$$

$$\boldsymbol{Q}_{ij}=(\boldsymbol{T}_{ji})^{-1}\boldsymbol{R}_{ij}^{vc}(\boldsymbol{I}-\boldsymbol{H}_{ij})\boldsymbol{D}_{ij}^{T}$$

Considering that $\boldsymbol{q}_j'=\boldsymbol{D}_{ij}\boldsymbol{q}_{ji}^{v}$, Eq. (34) can be written as

$$\boldsymbol{q}_j=\boldsymbol{P}_{ij}\boldsymbol{q}_i+\boldsymbol{Q}_{ij}\boldsymbol{q}_j' \tag{35}$$

Similarly, the constraint equations for joint J_{jk} are

$$\boldsymbol{q}_k=\boldsymbol{P}_{jk}\boldsymbol{P}_{ij}\boldsymbol{q}_i+\boldsymbol{P}_{jk}\boldsymbol{Q}_{ij}\boldsymbol{q}_j'+\boldsymbol{Q}_{jk}\boldsymbol{q}_k' \tag{36}$$

The constraint equations for all the rest joints can be formulated similar to Eq. (36). The constraint equations for the entire open-loop system can thus be integrated as

$$\boldsymbol{q}=\boldsymbol{B}'\boldsymbol{q}' \tag{37}$$

The open-loop constraint matrix $\boldsymbol{B}'$ takes the form

$$\boldsymbol{B}'=\begin{bmatrix}
\boldsymbol{I}_a & \boldsymbol{0} & \boldsymbol{0} & \boldsymbol{0} & \boldsymbol{0} & \boldsymbol{0} & \boldsymbol{0} & \boldsymbol{0} & \boldsymbol{0} & \boldsymbol{0} & \boldsymbol{0}\\
\boldsymbol{0} & \boldsymbol{I}_6 & \boldsymbol{0} & \boldsymbol{0} & \boldsymbol{0} & \boldsymbol{0} & \boldsymbol{0} & \boldsymbol{0} & \boldsymbol{0} & \boldsymbol{0} & \boldsymbol{0}\\
\boldsymbol{0} & \boldsymbol{0} & \boldsymbol{I}_b & \boldsymbol{0} & \boldsymbol{0} & \boldsymbol{0} & \boldsymbol{0} & \boldsymbol{0} & \boldsymbol{0} & \boldsymbol{0} & \boldsymbol{0}\\
\boldsymbol{0} & \boldsymbol{P}_{ij} & \boldsymbol{0} & \boldsymbol{Q}_{ij} & \boldsymbol{0} & \boldsymbol{0} & \boldsymbol{0} & \boldsymbol{0} & \boldsymbol{0} & \boldsymbol{0} & \boldsymbol{0}\\
\boldsymbol{0} & \boldsymbol{0} & \boldsymbol{0} & \boldsymbol{0} & \boldsymbol{I}_c & \boldsymbol{0} & \boldsymbol{0} & \boldsymbol{0} & \boldsymbol{0} & \boldsymbol{0} & \boldsymbol{0}\\
\boldsymbol{0} & \boldsymbol{P}_{jk}\boldsymbol{P}_{ij} & \boldsymbol{0} & \boldsymbol{P}_{jk}\boldsymbol{Q}_{ij} & \boldsymbol{0} & \boldsymbol{Q}_{jk} & \boldsymbol{0} & \boldsymbol{0} & \boldsymbol{0} & \boldsymbol{0} & \boldsymbol{0}\\
\boldsymbol{0} & \boldsymbol{0} & \boldsymbol{0} & \boldsymbol{0} & \boldsymbol{0} & \boldsymbol{0} & \boldsymbol{I}_d & \boldsymbol{0} & \boldsymbol{0} & \boldsymbol{0} & \boldsymbol{0}\\
\boldsymbol{0} & \boldsymbol{P}_{jm}\boldsymbol{P}_{ij} & \boldsymbol{0} & \boldsymbol{P}_{jm}\boldsymbol{Q}_{ij} & \boldsymbol{0} & \boldsymbol{0} & \boldsymbol{0} & \boldsymbol{Q}_{jm} & \boldsymbol{0} & \boldsymbol{0} & \boldsymbol{0}\\
\boldsymbol{0} & \boldsymbol{0} & \boldsymbol{0} & \boldsymbol{0} & \boldsymbol{0} & \boldsymbol{0} & \boldsymbol{0} & \boldsymbol{0} & \boldsymbol{I}_e & \boldsymbol{0} & \boldsymbol{0}\\
\boldsymbol{0} & \boldsymbol{P}_{mr}\boldsymbol{P}_{jm}\boldsymbol{P}_{ij} & \boldsymbol{0} & \boldsymbol{P}_{mr}\boldsymbol{P}_{jm}\boldsymbol{Q}_{ij} & \boldsymbol{0} & \boldsymbol{0} & \boldsymbol{0} & \boldsymbol{P}_{mr}\boldsymbol{Q}_{jm} & \boldsymbol{0} & \boldsymbol{Q}_{mr} & \boldsymbol{0}\\
\boldsymbol{0} & \boldsymbol{0} & \boldsymbol{0} & \boldsymbol{0} & \boldsymbol{0} & \boldsymbol{0} & \boldsymbol{0} & \boldsymbol{0} & \boldsymbol{0} & \boldsymbol{0} & \boldsymbol{I}_h
\end{bmatrix}$$

https://doi.org/10.1017/jmech.2011.51 Published online by Cambridge University Press

where $a = 6i - 6$, $b = 6(j - i - 1)$, $c = 6(k - j - 1)$, $d = 6(m - k - 1)$, $e = 6(r - m - 1)$, and $h = 6(n - r)$. The subscript of each identity matrix $\boldsymbol{I}$ denotes its dimension. Obviously, matrix $\boldsymbol{B}'$ contains information about all joints and reveals constraint topology of open-loop SR-MBS.

In Eq. (37), $\boldsymbol{q}'$ are the general displacements of open-loop SR-MBS, which are the combination of absolute displacements of CM of unconstrained bodies and absolute joint displacements of constrained bodies, *i.e.*,

$$\boldsymbol{q}' = \left[(\boldsymbol{q}_1')^T \quad (\boldsymbol{q}_2')^T \quad \cdots \quad (\boldsymbol{q}_n')^T \right]^T$$

where $\boldsymbol{q}_j' = \boldsymbol{D}_{ij}\, \boldsymbol{q}_{ji}^v$, $\boldsymbol{q}_k' = \boldsymbol{D}_{jk}\, \boldsymbol{q}_{kj}^v$, $\boldsymbol{q}_m' = \boldsymbol{D}_{jm}\, \boldsymbol{q}_{mj}^v$, $\boldsymbol{q}_r' = \boldsymbol{D}_{mr}\, \boldsymbol{q}_{rm}^v$, $\boldsymbol{q}_\varepsilon' = \boldsymbol{q}_\varepsilon$ ($\varepsilon = 1, 2, \cdots, n$ and $\varepsilon \neq j, k, m, r$).

Substitute Eq. (37) and its time derivation, *i.e.*, $\dot{\boldsymbol{q}} = \boldsymbol{B}'\dot{\boldsymbol{q}}'$, into Eqs. (30) ~ (32), it yields

$$\frac{\mathrm{d}}{\mathrm{d}t}\left(\frac{\partial T}{\partial \dot{\boldsymbol{q}}'^T} \right) = \boldsymbol{B}'^T \boldsymbol{M} \boldsymbol{B}' \ddot{\boldsymbol{q}}' = \boldsymbol{M}' \ddot{\boldsymbol{q}}' \tag{38}$$

$$\frac{\partial V}{\partial \boldsymbol{q}'^T} = \boldsymbol{B}'^T \boldsymbol{K} \boldsymbol{B}' \boldsymbol{q}' + \boldsymbol{B}'^T \boldsymbol{f}_g = \boldsymbol{K}' \boldsymbol{q}' + \boldsymbol{B}'^T \boldsymbol{f}_g \tag{39}$$

$$\boldsymbol{f}_d' = \frac{\partial P}{\partial \dot{\boldsymbol{q}}'^T} = \boldsymbol{B}'^T \boldsymbol{C} \boldsymbol{B}' \dot{\boldsymbol{q}}' = \boldsymbol{C}' \dot{\boldsymbol{q}}' \tag{40}$$

It then follows a minimal set of linearized ODEs for an open-loop SR-MBS

$$\boldsymbol{M}' \ddot{\boldsymbol{q}}' + \boldsymbol{C}' \dot{\boldsymbol{q}}' + \boldsymbol{K}' \boldsymbol{q}' = \boldsymbol{B}'^T (\boldsymbol{f}_e - \boldsymbol{f}_g) \tag{41}$$

where $\boldsymbol{M}'$, $\boldsymbol{C}'$ and $\boldsymbol{K}'$ are determined via the same quadric transformation

$$\boldsymbol{E}' = \boldsymbol{B}'^T \boldsymbol{E} \boldsymbol{B}' \quad (\boldsymbol{E} = \boldsymbol{M}, \boldsymbol{K}, \boldsymbol{C}) \tag{42}$$

Equation (41) can be regarded as obtained by multiplying Eq. (28) with $\boldsymbol{B}'^{\mathrm{T}}$ and replacing $\boldsymbol{q}$ by $\boldsymbol{B}'\boldsymbol{q}'$. It indicates that the solution of constraint equations for open-loop SR-MBS can be directly obtained via quadric transformation upon system matrices for free SR-MBS, by using the corresponding open-loop constraint matrix $\boldsymbol{B}'$.

4.3 Vibration Formulation of Closed-Loop SR-MBS

Considering closed-loop SR-MBS as shown in Fig. 3(e), similar to Eq. (33), the constraint equations for joint J_{kr} can be expressed as

$$\boldsymbol{H}_{kr}\, \boldsymbol{q}_{kr}^v = \boldsymbol{H}_{kr}\, \boldsymbol{q}_{rk}^v \tag{43}$$

where $\boldsymbol{q}_{kr}^v$ and $\boldsymbol{q}_{rk}^v$ denote the displacements of points Q_{kr} and Q_{rk} with respect to v_{kr}-$x''y''z''$, respectively.

Rewrite matrix $\boldsymbol{B}'$ with each six rows as a block, *i.e.*, $\boldsymbol{B}' = [\boldsymbol{B}_1'^{\mathrm{T}} \quad \boldsymbol{B}_2'^{\mathrm{T}} \quad \cdots \quad \boldsymbol{B}_n'^{\mathrm{T}}]^{\mathrm{T}}$. According to Eqs. (37) and (15) one can obtain $\boldsymbol{q}_{kr}^v = \boldsymbol{R}_{kr}^{cv} \boldsymbol{T}_{kr} \boldsymbol{B}_k'$ and $\boldsymbol{q}_{rk}^v = \boldsymbol{R}_{kr}^{cv} \boldsymbol{T}_{rk} \boldsymbol{B}'$. Then Eq. (43) can be rewritten as

$$\boldsymbol{H}_{kr}\, \boldsymbol{R}_{kr}^{cv} (\boldsymbol{T}_{kr}\, \boldsymbol{B}_k' - \boldsymbol{T}_{rk}\, \boldsymbol{B}_r')\, \boldsymbol{q}' = \boldsymbol{0} \tag{44}$$

If the number of cut-joints in a general spatial closed-loop SR-MBS is c, the constraint equations for all cut-joints can be integrated as

$$\boldsymbol{B}\boldsymbol{q}' = \boldsymbol{0} \tag{45}$$

where $\boldsymbol{B} = [\boldsymbol{B}_1^{\mathrm{T}} \quad \boldsymbol{B}_2^{\mathrm{T}} \quad \cdots \quad \boldsymbol{B}_c^{\mathrm{T}}]^{\mathrm{T}}$, and $\boldsymbol{B}_i$ is the coefficient matrix of constraint equations for the ith cut-joint.

Transmission mechanism can be treated as cut-joint. Suppose the constraints between body B_k and B_r in Fig. 3(e) is not a joint J_{kr} as mentioned before but a transmission mechanism T_{kr}. The details of T_{kr} can be seen in section 1. Similar to Eq. (44), constraint equations specified as Eq. (6) can be rewritten as

$$(\boldsymbol{G}_k\, \boldsymbol{R}_{jk}^{ck}\, \boldsymbol{T}_{kj}\, \boldsymbol{B}_k' + \boldsymbol{G}_r\, \boldsymbol{R}_{mr}^{cr}\, \boldsymbol{T}_{rm}\, \boldsymbol{B}_r')\, \boldsymbol{q}' = \boldsymbol{0} \tag{46}$$

If the number of transmission mechanisms in a general SR-MBS is t, the constraint equations for all transmission mechanisms can be integrated as

$$\boldsymbol{Z}\boldsymbol{q}' = \boldsymbol{0} \tag{47}$$

where $\boldsymbol{Z} = [\boldsymbol{Z}_1^T \quad \boldsymbol{Z}_2^T \quad \cdots \quad \boldsymbol{Z}_t^T]^T$, and $\boldsymbol{Z}_j$ is the coefficient matrix of constraint equations for the jth transmission mechanism.

Equation (45) and (47) can be integrated as constraint equations for cut-joints as follows

$$\begin{bmatrix} \boldsymbol{B} \\ \boldsymbol{Z} \end{bmatrix} \boldsymbol{q}' = \boldsymbol{0} \tag{48}$$

Since there might be redundant constraints in closed-loop system, Eq. (48) can be solved to form independent constraint equations

$$\tilde{\boldsymbol{q}}' = \tilde{\boldsymbol{B}}' \boldsymbol{q}'' \tag{49}$$

where $\boldsymbol{q}''$ is a vector of all independent variables in $\boldsymbol{q}'$, and $\tilde{\boldsymbol{q}}'$ is that of dependent ones.

Considering that the elements in $\boldsymbol{q}''$ or $\tilde{\boldsymbol{q}}'$ are not necessarily consecutive variables in $\boldsymbol{q}'$, they are reordered by introducing a matrix $\boldsymbol{S}$ as

$$\boldsymbol{q}' = \boldsymbol{S}[\boldsymbol{q}''^T \quad \tilde{\boldsymbol{q}}'^T]^T \tag{50}$$

Substituting Eq. (49) into Eq. (50), it yields

$$\boldsymbol{q}' = \boldsymbol{S} \begin{bmatrix} \boldsymbol{I} \\ \tilde{\boldsymbol{B}}' \end{bmatrix} \boldsymbol{q}'' = \boldsymbol{B}'' \boldsymbol{q}'' \tag{51}$$

Here we call matrix $\boldsymbol{B}''$ the cut-joint constraint matrix. Considering Eq. (37), one can obtain

$$\boldsymbol{q} = \boldsymbol{B}' \boldsymbol{q}' = \boldsymbol{B}' \boldsymbol{B}'' \boldsymbol{q}'' \tag{52}$$

https://doi.org/10.1017/jmech.2011.51 Published online by Cambridge University Press

Similar to formulation of open-loop SR-MBS, substitute Eq. (52) and its time derivation, *i.e.*, $\dot{\boldsymbol{q}} = \boldsymbol{B}'\boldsymbol{B}''\dot{\boldsymbol{q}}''$, into Eqs. (30) ~ (32), a minimal set of linearized ODEs for closed-loop SR-MBS can be expressed as

$$\boldsymbol{M}''\ddot{\boldsymbol{q}}'' + \boldsymbol{C}''\dot{\boldsymbol{q}}'' + \boldsymbol{K}''\boldsymbol{q}'' = \boldsymbol{B}''^{T}\boldsymbol{B}'^{T}(\boldsymbol{f}_e - \boldsymbol{f}_g) \tag{53}$$

where $\boldsymbol{M}''$, $\boldsymbol{C}''$ and $\boldsymbol{K}''$ are determined via the same quadric transformation

$$\boldsymbol{E}'' = \boldsymbol{B}''^{T}\boldsymbol{E}'\boldsymbol{B}'' = \boldsymbol{B}''^{T}\boldsymbol{B}'^{T}\boldsymbol{E}\boldsymbol{B}'\boldsymbol{B}'' \quad (\boldsymbol{E} = \boldsymbol{M}, \boldsymbol{K}, \boldsymbol{C}) \tag{54}$$

Equation (53) can be regarded as obtained by multiplying Eq. (41) with the transposed cut-joint constraint matrix $\boldsymbol{B}''^{\mathrm{T}}$ and replacing $\boldsymbol{q}'$ by $\boldsymbol{B}''\boldsymbol{q}''$. It indicates that the solution of constraint equations for cut-joints can be directly obtained via quadric transformation upon system matrices for open-loop system, by using the corresponding cut-joint constraint matrix $\boldsymbol{B}''$.

Complicated solving for constraints and linearization are unnecessary in this method, and the resulting equations contain explicitly the design parameters. The suggested method can be used to greatly simplify the procedure of vibration calculation. Furthermore, the suggested method is particularly suitable for sensitivity analysis and optimization for large-scale SR-MBS.

The proposed algorithm has been implemented in MATLAB, and is named as AMVA (Automatic Modeling for Vibration Analysis). The eigenvalue problem is solved using standard LAPACK routines. The flowchart of the proposed algorithm is illustrated in Fig. 4.

4.4 Comparison with Traditional Methods

The procedure of most of the conventional methods for vibration calculation can be concluded as follows. Firstly, the general-purpose nonlinear equations of motion, in most cases DAEs, are formulated in terms of coordinates of all bodies. Secondly, the Jacobian of constraint equations is calculated to transform DAEs into ODEs by eliminating the Lagrange's Multipliers. Thirdly, a minimal set of nonlinear ODEs in terms of independent generalized coordinates are obtained.

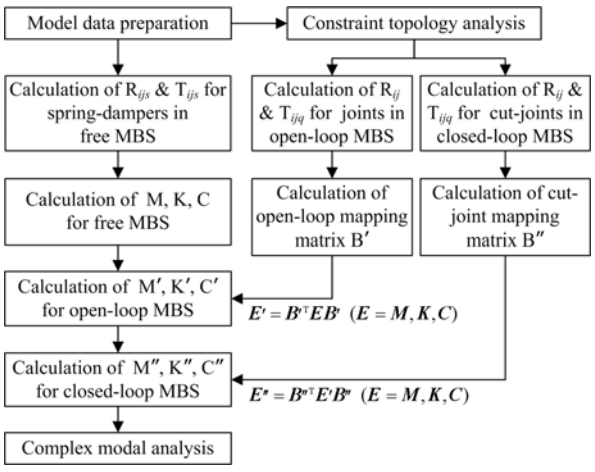


Fig. 4 Flowchart of the proposed formulation

Finally, the resulting equations are linearized at small vicinity near the equilibrium position. A large amount of computational efforts are required for computation of trigonometric functions, derivation and linearization. Many kinds of software such as ADAMS employ this kind of method for obtaining a minimal set of linear ODEs for vibration analysis.

As shown in Fig. 4, there are three steps in the proposed method to generate a minimal set of second-order linear ODEs for vibration calculation. Firstly, system matrices for linear ODEs of free system are directly generated by using linear transformation. Secondly, an open-loop constraint matrix is formulated to obtain linear ODEs for open-loop system. Finally, a cut-joint constraint matrix is solved to formulate a minimal set of second-order linear ODEs for closed-loop system.

Considering the definitions for vibration calculation, the major difference between the proposed method and previous studies lies in the definition and formulation of constraint equations. Conventionally, the constraint equations are defined in terms of coordinates of bodies or joints. The constraint equations and the Jacobian of constraint matrix are usually nonlinear ones. It is difficult, particularly for large-scale SR-MBS, to obtain the transformation matrix from the generalized coordinates to the independent coordinates. In this paper, however, the constraint equations are defined in terms of fine displacements of two acting points of the joint. The resulting linear constraint equations can be easily resolved to obtain the transformation matrix, *i.e.*, the open-loop constraint matrix and the cut-joint constraint matrix.

There are two major differences between the proposed method and most of the traditional methods. One is that the linearization is carried out before generating ODEs with small motion assumption which is satisfied for vibration. The other is that the formulation of a minimal set of second-order linear ODEs for constrained system is achieved by directly generating five matrices, *i.e.*, mass matrix, stiffness matrix and damping matrix for free system, an open-loop constraint matrix $\boldsymbol{B}'$ for open-loop system, and a cut-joint constraint matrix $\boldsymbol{B}''$ for closed-loop system.

Notice that Kang *et al*. have also proposed a similar method in which the linearization is carried out before generating ODEs with small motion assumption [30]. The results of system matrices for free system are actually the same as those derived by our method. The difference between Kang's method and ours lies in the formulation of a minimal set of ODEs for constrained system. They employ the partition of the Jacobian of constraint matrix, which is time-consuming to be obtained for SR-MBS with a large amount of constraints, to derive the relationship between generalized coordinates and the independent coordinates. We use the linear transformation matrix to directly formulate linearized constraint equations and then derive the relationship between generalized coordinates and the independent coordinates. Most of all, since the final system matrices can be directly obtained by only a few steps of matrices generation and multiplication, the computational efficiency can be significantly improved

https://doi.org/10.1017/jmech.2011.51 Published online by Cambridge University Press

for large-scale SR-MBS with a large amount of constraints.

The computational efficiency for vibration calculation can be significantly improved by using the proposed method, in comparison with most of the traditional approaches. An SR-MBS with n rigid bodies and m DOFs is taken as an example to demonstrate it. Suppose there are p constraints for the open-loop system and q ($p \le 6n - m \le q$) constraints for the entire system. There are mainly four factors that can help to improve the computational efficiency.

1. Relative small scale of matrix computation. Traditionally, a matrix with size $(12n - m) \times (12n - m)$ must be generated and solved to obtain system matrices with size $m \times m$. In addition, in order to express the $6n - m$ dependent coordinates in terms of m independent coordinates, it is necessary to get the inverse of a matrix with size $6n - m$, according to the method proposed in Ref. [30]. However, there are only matrices $\boldsymbol{M}$, $\boldsymbol{C}$, $\boldsymbol{K}$ with size $6n \times 6n$ and an open-loop constraint matrix $\boldsymbol{B}'$ with size $6n \times (6n - p)$ need to be easily generated for the proposed method. And then a cut-joint constraint matrix $\boldsymbol{B}''$ with size $(6n - p) \times m$ needs to be resolved to perform simple matrix multiplication for obtaining the final system matrices. In addition, there are only $6n - p - m$ dependent coordinates in terms of m independent coordinates, the size of matrix to be inversed is $6n - p - m$. It can be easily concluded that less computational efforts are required for the proposed method.
2. Reduction of trigonometric functions computing. Conventionally, the variations of coordinates and postures between two acting points of a connection, such as spring-damper or joint, are computed based on homogeneous transformation. Instead, the linear transformation in the proposed method can significantly reduce computational efforts due to calculation of trigonometric functions. Obviously, the more connections there are, the more computational efforts can be reduced.
3. Avoidance of complex calculation of Jacobian of constraint equation which usually contains many trigonometric functions. It is time-consuming for the calculation of Jacobian of a matrix with size $(6n - m) \times (6n - m)$. Instead, the constraint matrices $\boldsymbol{B}'$ and $\boldsymbol{B}''$ can be easily obtained by using the presented definition of constraints for the proposed method.
4. Avoidance of linearization of nonlinear equations of motion. The ODEs generated by conventional methods are nonlinear ones that need to be linearized before perform vibration calculation [6-10]. Instead, the ODEs obtained by using the proposed method are a minimal set of second-order linear ODEs which can be directly used for vibration calculation.

Besides the promise in improving the computational efficiency, the proposed method can be applied in sensitivity analysis because the resulting equations depend on the design parameters explicitly. As is known to all, the eigen-sensitivity is based on the derivatives of the system matrices, which are denoted as $\boldsymbol{M}''$, $\boldsymbol{C}''$ and $\boldsymbol{K}''$ in this paper, with respect to the design parameters [27,28]. Conventionally, the system matrices are solved numerically and they depend on the design parameters implicitly. Therefore the derivatives of the system matrices with respect to a certain parameter p are usually obtained by using finite difference method. However, it can be seen that each kind of design parameters can be easily traced in different system matrices obtained by using the proposed method. For example, the stiffness coefficients of spatial spring K_{ijs} only exist in matrix $\boldsymbol{K}_{ijs}^{u}$ in Eqs. (23) and (24) ($\boldsymbol{E}_{ijs}^{u}$ refers to $\boldsymbol{K}_{ijs}^{u}$ for spring). The position parameters of K_{ijs} exist in $\boldsymbol{T}_{ijs}$ and $\boldsymbol{T}_{jis}$, and its orientation parameters exist in $\boldsymbol{R}_{ijs}^{cu}$. Similarly, the position and orientation parameters of joint exist in $\boldsymbol{B}'$ and $\boldsymbol{B}''$. Therefore the derivatives $d\boldsymbol{M}''/dp$, $d\boldsymbol{C}''/dp$ and $d\boldsymbol{K}''/dp$ can be further derived analytically. For example, suppose that p is the mass or inertia parameter of body B_i, then

$$\frac{\partial \boldsymbol{M}''}{\partial p} = \boldsymbol{B}''^{T}\boldsymbol{B}'^{T}\,\mathrm{diag}\left(\mathbf{0} \;\cdots\; \mathbf{0} \;\; \frac{\partial \boldsymbol{M}_i}{\partial p} \;\; \mathbf{0} \;\cdots\; \mathbf{0}\right)\boldsymbol{B}'\boldsymbol{B}'' \tag{55}$$

The sensitivity formulation based on the proposed method will be investigated in the next step.

5. NUMERICAL EXPERIMENTS

In this section, numerical experiments were carried out to verify the correctness of the proposed method. It is unsuitable to compare straightforwardly the results of system matrices with theoretical solutions because these matrices are usually very large in size. Normal mode analysis (NMA), transfer function analysis (TFA) and time response analysis (TRA) for the same model were performed in AMVA and commercial software ADAMS. The results of natural frequencies, the damping ratios, and the transfer function, which are determined by eigenvalues and eigenvectors of the system, were compared to verify the correctness of the proposed method. A T-shape cantilever beam and a Stewart platform, which represent SR-MBS with tree and closed-loop topology, are selected as models.

5.1 T-Shape Cantilever Beam

As shown in Fig. 5, the size of the first and the second parts of a T-shape cantilever beam are 0.23m × 0.01m × 0.02m and 0.02m × 0.01m × 0.17m, and the material is steel. The flexible beam is modeled as n = 16 rigid bodies interconnected by spherical joint and spring-damper at the center of the cross-section. Therefore there are f = 48 DOFs for the tree SR-MBS model of the T-shape cantilever beam. The length, mass and inertia tensor of each body are l_i = 0.025m, m_i = 0.26kg and $\boldsymbol{J}_i$ = diag(0.11 6.11 6.04) × 10^{-4}kg·m^2,

https://doi.org/10.1017/jmech.2011.51 Published online by Cambridge University Press

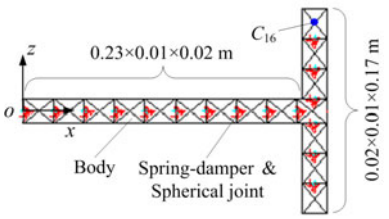


Fig. 5 Tree SR-MBS model of a *T*-shape cantilever beam

respectively. The torsion stiffness and damping coefficients of each spring-damper are $[k_\alpha^k \ k_\beta^k \ k_\gamma^k] = [1.59 \ 5.81 \ 1.50] \times 10^4 \text{N·m·rad}^{-1}$ and $[c_\alpha^k \ c_\beta^k \ c_\gamma^k] = [0.84 \ 3.74 \ 1.61] \times 10^{-2} \text{N·m·s·rad}^{-1}$. The y-axis of the local frame of each spring-damper is parallel to the *y*-axis of the global frame, and the *z*-axis of the local frame of each spring-damper is normal to the cross- section.

Normal mode analysis (NMA), transfer function analysis (TFA) and time response analysis (TRA) on the SR-MBS model by using AMVA and ADAMS are compared to verify the proposed method. The same vibration calculations on a FEM model of the cantilever beam, with 10694 nodes and 6375 elements of solid tetrahedron, are also performed in NASTRAN to verify the accuracy to the SR-MBS model.

The natural frequencies of the SR-MBS model solved by AMVA and ADAMS are shown in Fig. 6. Comparisons show that the maximal and mean relative error between natural frequencies solved by AMVA and results of ADAMS are 1.48×10^{-4} and 1.70×10^{-5}. It indicates that the results of eigenvalue calculated by using AMVA and ADAMS are identical except very tiny numerical errors. The accuracy of the SR-MBS model depends on how many rigid bodies are used to simulate the flexibility of the beam. The differences between the first ten natural frequencies of the present SR-MBS model and the FEM model are negligible. It can be concluded that if the flexible body in a mechanical system is properly modeled as a set of SR- MBS, the proposed method can also be used for vibration calculation of the system under working conditions.

Transfer functions analysis on the SR-MBS model is performed both in AMVA and ADAMS. The swept sine exciting force and the displacement response are both set in *y*-direction at C_{16}, *i.e.*, CM of body B_{16}. Comparisons in Fig. 7 show that solutions of transfer function calculated by using AMVA coincide well with the results solved in ADAMS. The maximal and mean relative errors of magnitude of the transfer function are 2.73×10^{-4} and 4.65×10^{-5}. It can be concluded that the proposed method can be used for vibration calculation of tree SR-MBS. Transfer functions analysis on the FEM model is also performed in NASTRAN and the results are presented in Fig. 7. There are only very small differences in high frequency domain between transfer function of the SR-MBS model and that of the FEM model.

Time response analysis on the SR-MBS model is performed both in AMVA and ADAMS. The swept

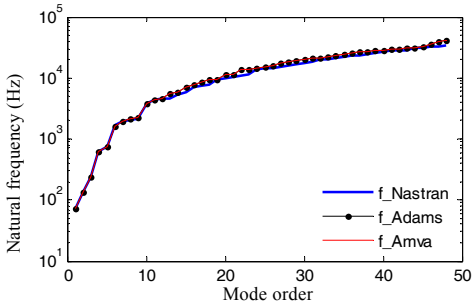


Fig. 6 Comparison of NMA results for the *T*-shape cantilever beam

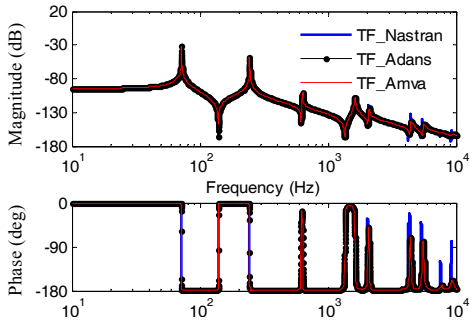


Fig. 7 Comparison of TFA solutions for the *T*-shape cantilever beam

sine force $f = 34.66\sin(4000\pi t^2)$ is applied on C_{16} in *y*-direction. The displacement responses of C_{16} in *y*-direction resolved by AMVA and ADAMS are shown in Fig. 8. It can be seen that solutions of time response calculated by using AMVA coincide well with the results solved in ADAMS. The maximal displacement in this case is 3.21×10^{-3}m. The maximal and mean errors of results in AMVA with respect to solutions in ADAMS are 3.03×10^{-5}m and 1.82×10^{-7}m. It can be concluded that the proposed method can be used for time response calculation of tree SR-MBS under vibratory status. The results of time response analysis on the FEM model are also presented in Fig. 8. It can be seen that the difference between time response of the SR-MBS model and that of the FEM model is negligible.

5.2 Stewart Isolation Platform

The proposed method has also been applied in vibration calculation of a Stewart isolation platform, which is modeled as a closed-loop SR-MBS. As shown in Fig. 9, the isolated platform is suspended on the fixed base via six parallel linear actuators. The upper and bottom ends of each linear actuator are connected to the isolated platform and the base, respectively, via flexible joints. Based on previous finite element analysis, each flexible joint is modeled as a spherical joint combined with three-dimensional torsion spring-damper. Each linear actuator is modeled as two rigid links connected by a cylindrical joint and a linear spring-damper along the axial direction of the link. Therefore there are $n = 14$ rigid bodies and $f = 18$ DOFs for the closed-loop

https://doi.org/10.1017/jmech.2011.51 Published online by Cambridge University Press

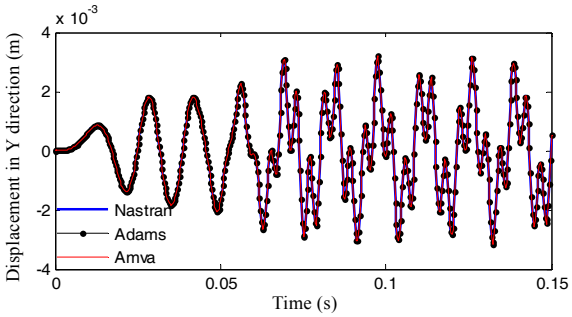


Fig. 8 Comparison of TRA solutions for the *T*-shape cantilever beam

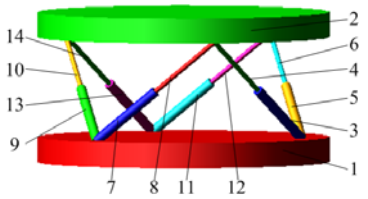


Fig. 9 Closed-loop SR-MBS model of a Stewart isolation platform

SR-MBS of the Stewart isolation platform. The parameters of bodies are shown in Table 3. Due to symmetrical configuration of six linear actuators, only parameters for one of them are shown in the table. The stiffness and damping coefficients of linear actuator are $k = 1.13 \times 10^5 \text{N·m}^{-1}$ and $c = 6.82 \times 10^2 \text{N·s·m}^{-1}$. The torsion stiffness and torsion damping coefficients of the flexible joint are $[k_\alpha \ k_\beta \ k_\gamma] = [2.01 \ 2 \ 1.76] \times 10^2 \text{N·m·rad}^{-1}$ and $[c_\alpha \ c_\beta \ c_\gamma] = [4.07 \ 4.05 \ 5.13] \times 10^{-2} \text{N·m·s·rad}^{-1}$. The coordinates of connections between base 1 and link 3 are designated as $\bar{\boldsymbol{r}}_{1,3} = [0.5 \ 0.1 \ 0]\,\text{m}$. The coordinates of connections between platform 2 and link 4 are designated as $\bar{\boldsymbol{r}}_{2,4} = [0.25 \ 0.5 \ 0.433]\,\text{m}$. The coordinates of connections between link 3 and link 4 are designated as $\bar{\boldsymbol{r}}_{3,4} = [0.375 \ 0.3 \ 0.2165]\,\text{m}$. The rest may be deduced by analogy, according to symmetrical configuration.

Normal mode analysis and transfer function analysis were both performed in ADAMS and AMVA to acquire vibration isolation performance of such a Stewart isolation platform. Natural frequencies and damping ratio solved in AMVA and ADAMS are compared in Fig. 10. The maximal and mean relative error of natural frequencies solved by AMVA with respect to results of ADAMS are 2.51×10^{-4} and 7.20×10^{-5}, and the maximal and mean relative error of damping ratio are 2.34×10^{-4} and 7.10×10^{-5}. It indicates that the results of eigenvalue calculated by using AMVA and ADAMS are identical except very tiny numerical errors. The swept sine exciting force and the displacement response are both set on the isolated platform at position with absolute coordinate $\bar{\boldsymbol{r}} = [0.25 \ 0.6 \ 0.433]\,\text{m}$ and in *y*-direction. Figure 11 shows that the maximal and

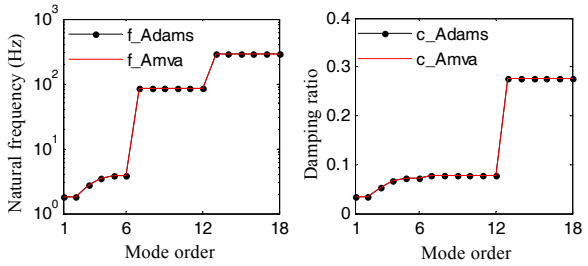


Fig. 10 Comparison of NMA results for the Stewart isolation platform

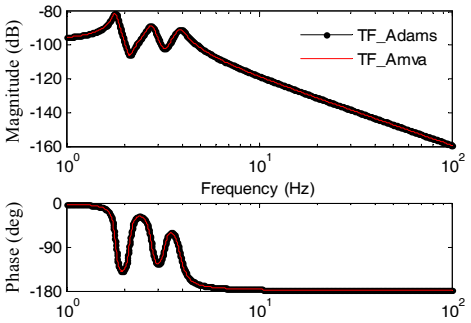


Fig. 11 Comparison of TFA solutions for the Stewart isolation platform

Table 3 Parameters of bodies in the Stewart isolation platform

No.	Mass (kg)	Inertia tensor $[I_{xx} \ I_{yy} \ I_{zz} \ I_{xy} \ I_{xz} \ I_{yz}]$ (kg·m^2)	Position & orientation of CM (m & rad)
1	3.92×10^2	$[3.14 \ 1.60 \ 1.60 \ 0 \ 0 \ 0] \times 10^1$	[0 0.05 0 1.571 1.571 0]
2	8.82×10^2	$[1.59 \ 0.80 \ 0.80 \ 0 \ 0 \ 0] \times 10^2$	[0 0.55 0 1.571 1.571 0]
3	1.213	$[4.63 \ 4.63 \ 0.17 \ 0.02 \ 0 \ 0] \times 10^{-3}$	[–0.345 0.19 0 –1.571 –0.464 –1.571]
4	0.546	$[2.28 \ 2.28 \ 0.027 \ 0 \ 0.01 \ 0] \times 10^{-3}$	[–0.450 0.40 0 –1.571 –0.464 –1.571]

mean relative errors of magnitude of the transfer function are 2.43×10^{-3} and 3.45×10^{-4}. It indicates that the proposed method can also be used for vibration calculation of closed-loop SR-MBS.

Time response analysis is also performed both in AMVA and ADAMS. The swept sine force $f = 2000\sin(400\pi t^2)$ is applied on the isolated platform at position with absolute coordinates $\bar{r} = [0.25 \ 0.6 \ 0.433]\text{m}$ along *y*-direction. The displacement responses of the same position in *y*-direction resolved by AMVA and ADAMS are shown in Fig. 12. It can be seen that solutions of time response calculated by using AMVA coincide well with the results solved in ADAMS. The maximal displacement in this case is $6.823 \times 10^{-3}\text{m}$. The maximal and mean errors are $2.55 \times 10^{-5}\text{m}$ and $2.93 \times 10^{-7}\text{m}$. It can be concluded that the proposed method can be used for time response calculation of closed-loop SR-MBS under vibratory status.

https://doi.org/10.1017/jmech.2011.51 Published online by Cambridge University Press

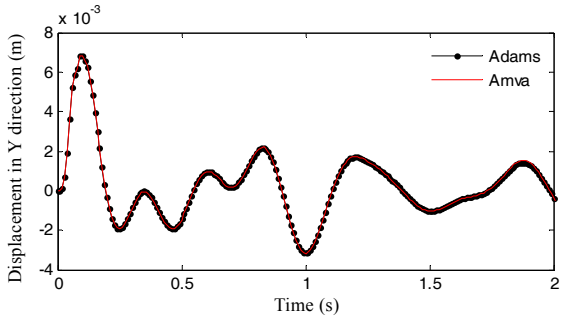


Fig. 12 Comparison of TRA solutions for the Stewart isolation platform

6. CONCLUSIONS

A new formulation based on constraint-topology transformation is proposed to generate oscillatory differential equations for a general SR-MBS. The dynamics of constraints are formulated via matrix generation and quadric transformation in three steps. Complicated solving for constraints and linearization are unnecessary for the proposed method, therefore the procedure of vibration calculation can be greatly simplified. The correctness of the proposed method is verified via numerical experiments on SR-MBS with open-loop and closed-loop topology. The proposed method can be used to greatly improve the computational efficiency for vibration calculation of large-scale SR-MBS.

Since the resulting equations depend on the design parameters explicitly, the suggested method is quite suitable for sensitivity analysis and optimization for large-scale SR-MBS, which is usually difficult from the conventional approaches.

ACKNOWLEDGEMENTS

The work has been supported by the National Basic Research Program of China (Grant No. 2009CB724205), and the National High Technology Research and Development Program of China (Grant No. 2009AA04Z148).

REFERENCES

1. Flores, P., Ambrósio, J., Claro, P. and Lankarani, H. M., "Kinematics and Dynamics of Multibody Systems with Imperfect Joints: Models and Case Studies, Springer-Verlag," *Berlin, Germany*, pp. 24–25 (2008).
2. Wittbrodt, E., Adamiec-Wójcik, I. and Wojciech, S., "Dynamics of Flexible Multibody Systems: Rigid Finite Element Method, Springer-Verlag," *Berlin, Germany*, pp. 37–45 (2006).
3. Wittenburg, J., "Dynamics of Multibody Systems, Springer-Verlag," *Berlin, Germany*, pp. 162–192 (2008).
4. Schiehlen, W., Guse, N. and Seifried, R., "Multibody Dynamics in Computational Mechanics and Engineering Applications," *Computer Methods in Applied Mechanics and Engineering*, **195**, pp. 5509–5522 (2006).
5. Laulusa, A. and Bauchau, O. A., "Review of Classical Approaches for Constraint Enforcement in Multibody Systems," *Journal of Computational and Nonlinear Dynamics*, **3**, pp. 011004 (2008).
6. Pott, A., Kecskeméthy, A. and Hiller, M., "A Simplified Force-based Method for the Linearization and Sensitivity Analysis of Complex Manipulation Systems," *Mechanism and Machine Theory*, **42**, pp. 1445–1461 (2007).
7. Cruz, H. D, Biscay, R. J., Carbonell, F., Ozaki, T. and Jimenez, J. C., "A Higher Order Local Linearization Method for Solving Ordinary Differential Equations," *Applied Mathematics and Computation*, **185**, pp. 197–212 (2007).
8. Negrut, D. and Ortiz, J. L., "A Practical Approach for the Lnearization of the Constrained Multibody Dynamics Equations," *Journal of Computational and Nonlinear Dynamics*, **1**, pp. 230–239 (2006).
9. Minaker, B. and Frise, P., "Linearizing the Equations of Motion for Multibody Systems Using an Orthogonal Complement Method," *Journal of Vibration and Control*, **11**, pp. 51–66 (2005).
10. Roy, D. and Kumar, R., "A Multi-step Transversal Linearization (MTL) Method in Non-linear Structural Dynamics," *Journal of Sound and Vibration*, **287**, pp. 203–226 (2005).
11. Wasfy, T. M. and Noor, A. K., "Computational Strategies for Flexible Multibody Systems," *Applied Mechanics Review*, **56**, pp. 553–613 (2003).
12. McPhee, J. J. and Redmond, S. M., "Modelling Multibody Systems with Indirect Coordinates," *Computer Methods in Applied Mechanics and Engineering*, **195**, pp. 6942–6957 (2006).
13. Liu, J. Y., Hong, J. Z. and Cui, L., "An Exact Nonlinear Hybrid-coordinate Formulation for Flexible Multibody Systems," *Acta Mechanica Sinica*, **23**, pp. 699–706 (2007).
14. Valasek, M., Sika, Z. and Vaculin, O., "Multibody Formalism for Real-time Application Using Natural Coordinates and Modified State Space," *Multibody System Dynamics*, **17**, pp. 209–227 (2007).
15. Attia, H. A., "Modelling of Three-dimensional Mechanical Systems Using Point Coordinates with a Recursive Approach," *Applied Mathematical Modelling*, **32**, pp. 315–326 (2008).
16. Amirouche, F., Fundamentals of Multibody Dynamics: Theory and Applications, Boston: Birkhauser, pp. 225–316 (2006).
17. Eberhard, P. and Schiehlen, W., "Computational Dynamics of Multibody Systems: History, Formalisms, and Applications," *Journal of Computational and Nonlinear Dynamics*, **1,** pp. 3–12 (2006).
18. Richard, M. J., McPhee, J. J. and Anderson, R. J.,

https://doi.org/10.1017/jmech.2011.51 Published online by Cambridge University Press

"Computerized Generation of Motion Equations Using Variational Graph-theoretic Methods," *Applied Mathematics and Computation*, **192**, pp. 135–156 (2007).
19. Rui, X. T., Wang, G. P., Lu, Y. Q. and Yun, L. F., "Transfer Matrix Method for Linear Multibody System," *Multibody System Dynamics*, **19**, pp. 179–207 (2008).
20. Van Keulen, F., Haftk, R. T. and Kim, N. H., "Review of Options for Structural Design Sensitivity Analysis. Part 1: Linear Systems," *Computer Methods in Applied Mechanics and Engineering*, **194**, pp. 3213–3243 (2005).
21. Ding, J. Y., Pan, Z. K. and Chen, L. Q., "Second Order Adjoint Sensitivity Analysis of Multibody Systems Described by Differential-algebraic Equations," *Multibody System Dynamics*, **18**, pp. 599–617 (2007).
22. Choi, K. M., Jo, H. K., Kim, W. H. and Lee, I. W., "Sensitivity Analysis of Non-conservative Eigensystems," *Journal of Sound and Vibration*, **274**, pp. 997–1011 (2004).
23. Xu, Z. H., Zhong, H. X., Zhu, X. W. and Wu, B. S., "An Efficient Algebraic Method for Computing Eigensolution Sensitivity of Asymmetric Damped Systems," *Journal of Sound and Vibration*, **327**, pp. 584–592 (2009).
24. Sliva, G., Brezillon, A., Cadou, J. M. and Duigou, L., "A Study of the Eigenvalue Sensitivity by Homotopy and Perturbation Methods," *Journal of Computational and Applied Mathematics*, **234**, pp. 2297–2302 (2010).
25. Jiang, W., Chen, X. D. and Yan, T. H., "Symbolic Formulation of Rigid Multibody Systems for Vibration Analysis based on Matrix Transformation," *Chinese Journal of Mechanical Engineering*, Chinese Ed., **44**, pp. 54–60 (2008).
26. Jiang, W., Chen, X. D., Luo, X. and Huang, Q. J., "Symbolic Formulation of Large-scale Open-loop Multibody Systems for Vibration Analysis Using Absolute Joint Coordinates," *Journal of System Design and Dynamics*, **2**, pp. 1015–1026 (2008).
27. Lee, I. W., Kim, D. O. and Jung, G. H., "Natural Frequency and Mode Shape Sensitivities of Damped Systems: Part I, Distinct Natural Frequencies," *Journal of Sound and Vibration*, **223**, pp. 399–412 (1999).
28. Lee, I. W., Kim, D. O. and Jung, G. H., "Natural Frequency and Mode Shape Sensitivities of Damped Systems: Part II, Multiple Natural Frequencies," *Journal of Sound and Vibration*, **223**, pp. 413–424 (1999).
29. Müller, A., "Elimination of Redundant Cut Joint Constraints for Multibody System Models," *Journal of Mechanical Design*, **126**, pp. 488–494 (2004).
30. Kang, J. S., Bae, S., Lee, J. M. and Tak, T. O., "Force Equilibrium Approach for Linearization of Constrained Mechanical System Dynamics," *Journal of Mechanical Design*, ASME, **125**, PP. 143–149 (2003).

(Manuscript received July 6, 2010,
accepted for publication November 25, 2010.)

https://doi.org/10.1017/jmech.2011.51 Published online by Cambridge University Press